

Characterizing the Connectome in Schizophrenia With Diffusion Spectrum Imaging

Alessandra Griffa,^{1,2*} Philipp Sebastian Baumann,^{3,4,5} Carina Ferrari,^{3,5}
Kim Quang Do,^{3,5} Philippe Conus,^{4,5} Jean-Philippe Thiran,^{1,2} and
Patric Hagmann^{1,2}

¹Signal Processing Laboratory 5 (LTS5), École Polytechnique Fédérale de Lausanne (EPFL),
Lausanne, Switzerland

²Department of Radiology, Centre Hospitalier Universitaire Vaudois (CHUV) and University
of Lausanne (UNIL), Lausanne, Switzerland

³Center for Psychiatric Neuroscience, Centre Hospitalier Universitaire Vaudois (CHUV) and
University of Lausanne (UNIL), Lausanne, Switzerland

⁴Service of General Psychiatry, Centre Hospitalier Universitaire Vaudois (CHUV) and
University of Lausanne (UNIL), Lausanne, Switzerland

⁵Department of Psychiatry, Centre Hospitalier Universitaire Vaudois (CHUV) and University
of Lausanne (UNIL), Lausanne, Switzerland

Abstract: Schizophrenia is a complex psychiatric disorder characterized by disabling symptoms and cognitive deficit. Recent neuroimaging findings suggest that large parts of the brain are affected by the disease, and that the capacity of functional integration between brain areas is decreased. In this study we questioned (i) which brain areas underlie the loss of network integration properties observed in the pathology, (ii) what is the topological role of the affected regions within the overall brain network and how this topological status might be altered in patients, and (iii) how white matter properties of tracts connecting affected regions may be disrupted. We acquired diffusion spectrum imaging (a technique sensitive to fiber crossing and slow diffusion compartment) data from 16 schizophrenia patients and 15 healthy controls, and investigated their weighted brain networks. The global connectivity analysis confirmed that patients present disrupted integration and segregation properties. The nodal analysis allowed identifying a distributed set of brain nodes affected in the pathology, including hubs and peripheral areas. To characterize the topological role of this affected core, we investigated the brain network shortest paths layout, and quantified the network damage after targeted attack toward the affected core. The centrality of the affected core was compromised in patients. Moreover the connectivity strength within the affected core, quantified with generalized fractional anisotropy and apparent

Additional Supporting Information may be found in the online version of this article.

Contract grant sponsor: Swiss National Science Foundation; Contract grant numbers: 320030_130090 (P.H. and A.G.), 320030_122419 (P.C. and K.Q.D.); Contract grant sponsor: National Center of Competence in Research (NCCR) “SYNAPSY—The Synaptic Bases of Mental Diseases”; Contract grant number: 51AU40_125759; Contract grant sponsor: Leenaards Foundation (P.H.); Contract grant sponsor: Center for Biomedical Imaging (CIBM) of the Geneva and Lausanne Universities.

*Correspondence to: Alessandra Griffa, École polytechnique fédérale de Lausanne (EPFL), Signal Processing Laboratory 5 (LTS5), EPFL STI IEL LTS5, ELD 233 (Bâtiment ELD), Station 11, Lausanne, Switzerland 1015. E-mail: alessandra.griffa@epfl.ch

Received for publication 17 March 2014; Revised 26 August 2014; Accepted 3 March 2014.

DOI: 10.1002/hbm.22633

Published online 12 September 2014 in Wiley Online Library (wileyonlinelibrary.com).

diffusion coefficient, was altered in patients. Taken together, these findings suggest that the structural alterations and topological decentralization of the affected core might be major mechanisms underlying the schizophrenia dysconnectivity disorder. *Hum Brain Mapp* 36:354–366, 2015. © 2014 Wiley Periodicals, Inc.

Key words: psychosis; brain network; diffusion spectrum imaging; graph theory; magnetic resonance imaging; schizophrenia; connectome

INTRODUCTION

Schizophrenia is a major psychiatric disorder characterized by disabling positive, negative, and cognitive symptoms. According to the dysconnectivity hypothesis [Friston and Frith, 1995], distributed alterations of brain connectivity patterns, and abnormal functional integration between distinct brain areas could underlie the symptoms observed in the pathology [Stephan et al., 2006, 2009]. Indeed a remarkable number of studies based on magnetic resonance imaging (MRI) highlighted morphological [Glahn et al., 2008; Honea et al., 2005] and connectivity [Fitzsimmons et al., 2013; Pettersson-Yeo et al., 2011] disturbances of distributed brain regions, with particular involvement of frontal, parietal, and temporal cortices, subcortical structures, bilaterally but more predominantly on the left hemisphere [Bora et al., 2011; Canu et al., 2014; Ellison-Wright and Bullmore, 2009; Shepherd et al., 2012].

The connectome framework [Hagmann Patric, 2005; Sporns et al., 2005] describes the brain connectivity network in terms of graph measures, and therefore, proves to be ideally suited for the investigation of a dysconnectivity disease like schizophrenia [Bullmore and Sporns, 2009; Filippi et al., 2013; Guye et al., 2010]. Particularly, this framework allows quantifying and comparing network integration and segregation properties that underlie distributed information processing and functional specialization [Bullmore and Bassett, 2011; Meskaldji et al., 2013; Sporns, 2013; Varoquaux and Craddock, 2013], and could provide a more insightful picture of brain alterations occurring in schizophrenia [Canu et al., 2014]. A growing number of studies combined a graph theory approach with functional MRI, diffusion MRI, or cortical thickness correlation analysis to investigate brain network alterations occurring in schizophrenia [Fornito et al., 2012; Griffa et al., 2013; Lynall et al., 2010; van den Heuvel and Fornito, 2014]. Studies adopting graph theory reported alterations of the structural and functional brain topology in schizophrenia, pointing out a less efficient network organization and a limited capacity of functional integration. To our knowledge, no diffusion-based study on schizophrenia used diffusion spectrum imaging (DSI) technique.

A decrease of brain network efficiency, associated with a reduced capacity of integration of information between brain areas, is a robust finding from anatomical connectivity studies [Fornito et al., 2012; van den Heuvel and Fornito, 2014].

Various structural substrates have been proposed to underlie the brain network efficiency loss occurring in schizophrenia. Passing from the analysis of global network properties to the role of individual nodes, different brain cores have been shown to be involved in the pathology. Applying a network based statistics approach, Zalesky and colleagues identified a distributed fronto-parietal / occipital network as possible substrate of global network alterations [Zalesky et al., 2011]. Default mode network (DMN) regions were also shown to be involved in the pathology [Skudlarski et al., 2010; Zhang et al., 2012].

A common element among reported core-damages in schizophrenia is the presence of brain network hubs. Global network alterations can indeed be associated to a distributed weakening of hub regions, and specially prefrontal, limbic, temporal, and parietal areas [van den Heuvel et al., 2010; Wang et al., 2012; Zhang et al., 2012]. Brain hubs are nodes presenting a high degree of centrality in the brain communication network, and have, therefore, been associated to a considerable metabolic cost and a potential higher vulnerability in the context of psychiatric disorders [Bullmore and Sporns, 2012]. Brain connections between a specific set of hub regions, the rich-club [van den Heuvel and Sporns, 2011], have recently been shown to be weakened in schizophrenia compared to controls, and compared to connections between other brain areas [van den Heuvel et al., 2013]. The involvement of the rich-club has as well been underlined by functional studies on schizophrenia [Yu et al., 2013], and diffusion MRI studies on schizophrenia siblings [Collin et al., 2013] and 22q11 deletion syndrome (considered a genetic subtype of schizophrenia) [Ottet et al., 2013].

Even though a large amount of evidence points toward an alteration of normal hub cores in schizophrenia and to an affection of the related connections disproportionate to other brain tracts, this effect may not necessarily be specific to schizophrenia neuropathology only [Rubinov and Bullmore, 2013], considering that high degree nodes have been implicated in different brain pathologies [Drzezga et al., 2011; Griffa et al., 2013; Lo et al., 2010; Zhang et al., 2011] and normal aging [Damoiseaux et al., 2009; Tomasi and Volkow, 2012].

In schizophrenia, losses of overall brain network properties have been extensively associated to hubs and rich-club disruption [Rubinov and Bullmore, 2013; van den Heuvel and Fornito, 2014]; to alterations of brain network hierarchical organization [Bassett et al., 2008]; to disruption of

anatomical connections among fronto-parietal-occipital areas [Zalesky et al., 2011] and fronto-temporal poles [van den Heuvel et al., 2010], DMN [Skudlarski et al., 2010], and to long associative fasciculi [Canu et al., 2014]. Taken together these findings corroborate the hypothesis that schizophrenia is associated to a widespread rather than localized alteration of brain structural connectivity, implying a modified organization of the brain communication system that involves high degree cores.

Building on these considerations, this study aims to investigate core damages and specific brain network topological features underlying the connectome disruption observed in schizophrenia, and to quantitatively characterize such alterations. Particularly, we propose that the decentralization of a distributed set of regions within the brain network is a possible mechanism underlying the schizophrenia pathology. Brain connectivity networks were estimated from DSI data for 16 chronic schizophrenia patients and 15 healthy controls. DSI is characterized by strong diffusion weighting and high angular resolution. As a consequence DSI is more sensitive and specific than classical diffusion tensor imaging to white matter microstructural organization, crossing-fibers can be mapped accurately and tissue alterations affecting the slow diffusion compartment may be captured [Baumann et al., 2012; Mendelsohn et al., 2006; Wedeen et al., 2012].

As a first step, global and nodal integration and segregation network properties were assessed to corroborate previous findings [Bassett et al., 2008; van den Heuvel et al., 2010; Wang et al., 2012; Zalesky et al., 2011]. Thereafter, alterations of nodal properties allowed identifying a distributed core affected in schizophrenia, in substantial agreement with previous studies [van den Heuvel and Fornito, 2014]. More importantly, the topological role of the affected core within the overall brain connectivity patterns was assessed in a graph theoretical framework, to characterize brain organizational principles underlying the pathology.

METHODS AND MATERIALS

Subjects

Sixteen patients were recruited from the outpatient clinic of the department of psychiatry, Lausanne University Hospital, Switzerland, and met criteria DSM-IV for schizophrenia or schizoaffective disorder [American Psychiatric Association, 2000]. Fifteen age, gender, and handedness matched healthy controls were assessed with the Diagnostic Interview for Genetic Studies [Preisig et al., 1999]. Subjects with major mood, psychotic, or substance-use disorders and having first-degree relative with a psychotic disorder were excluded. Moreover, a history of neurological disease was an exclusion criterion for all subjects.

Mean age for patients was 42.0 ± 10.1 years; mean age for controls was 41.1 ± 9.6 years. No statistical difference in age, gender, and handedness was present between the two groups (Supporting Information Table S1). Fourteen of

the 16 patients were taking medication at the time of this study, with an average medication of 341 ± 202 mg chlorpromazine equivalent dose (CPZ) [Andreasen et al., 2010].

Informed written consent in accordance with our institutional guidelines (protocol approved by the Ethic Committee of Clinical Research of the Faculty of Biology and Medicine, University of Lausanne, Switzerland) was obtained all the subjects.

Magnetic Resonance Imaging

MRI sessions were performed on a 3 Tesla scanner (Magnetom TrioTim, Siemens Medical Solutions), equipped with a 32-channel head coil. Each scanning session included a magnetization-prepared rapid acquisition gradient echo (MPRAGE) sequence with 1 mm in-plane resolution and 1.2 mm slice thickness, covering $240 \times 257 \times 160$ voxels. The TR, TE and TI were, respectively, 2,300, 2.98, and 900 ms. The DSI sequence included 128 diffusion-weighted images with a maximum b -value of $8,000 \text{ s/mm}^2$ and one b_0 reference image. The acquisition volume was made of $96 \times 96 \times 34$ voxels with $2.2 \times 2.2 \times 3$ mm resolution. TR and TE were 6,100 and 144 ms, respectively. The acquisition time of the DSI sequence was 13 min and 27 s. DSI datasets were visually inspected for signal drop-outs across the scanning time. Signal drop-outs are linked to motion artifacts [Yendiki et al., 2014]. None of the investigated subjects presented important signal drop-outs and needed to be excluded from this study.

Brain Network Estimation

Weighted, undirected (symmetric) structural connectivity matrices were estimated combining diffusion and morphological MRI data, and using the Connectome Mapping Toolkit [Cammoun et al., 2012; Daducci et al., 2012; Hagmann et al., 2010b]. MPRAGE volumes were segmented into white matter, grey matter, and cerebrospinal fluid compartments, and linearly registered to the b_0 volume. Thereafter, the grey matter volume was subdivided into 68 cortical and 14 subcortical anatomical regions, according to the Desikan–Killiany atlas [Desikan et al., 2006], and defining $N = 82$ brain network nodes. DSI data were reconstructed according to [Wedeen et al., 2005], allowing to estimate multiple diffusion directions per voxel. Deterministic streamline tractography [Mori et al., 1999] was performed on DSI reconstructed data, initiating 32 streamline propagations per voxel, per diffusion direction. The structural connectivity between each pair of grey matter nodes was then quantified as normalized connection density, defined as follows:

$$w_{uv} = \frac{1}{W} d_{uv} = \frac{1}{W} \left(\frac{2}{S_u S_v} \sum_{f \in F_{uv}} l(f) \right)$$

with w_{uv} connectivity strength associated to the edge connecting nodes u and v , W normalization factor, and d_{uv}

connection density between nodes u and v as defined in [Hagmann et al., 2008] (Supporting Information Fig. S1). Specifically, S_u and S_v indicate the surfaces of the brain regions u and v , $f \in F_{uv}$ a streamline belonging to the set F_{uv} of streamlines connecting regions u and v , and $l(f)$ the length of streamline f . The normalization by the streamline length is motivated by the fact that the number of streamline propagation seeds per brain connection is proportional to the average length of the streamlines belonging to the connection [Hagmann et al., 2008]. No between-group difference was present in terms of average streamline length (Supporting Information Table S2). The normalization reestablishes a more plausible and on average inverse relationship [Gigandet et al., 2013; Oh et al., 2014] between the connection length and the connectivity strength (Supporting Information Fig. S2). Main analyses were replicated without performing the normalization by the streamline length (Supporting Information Fig. S3).

From now on when we refer to the number of streamlines connecting two brain regions, we refer to its normalized version n_{uv}

$$n_{uv} = \sum_{f \in F_{uv}} \frac{1}{l(f)}$$

The normalization factor W was defined as the sum of the connection density values over all the edges belonging to the subject-wise connectivity matrix:

$$W = \sum_{u \in N} \sum_{v \in N, u \neq v} d_{uv}$$

Consequently, the weight of each edge represents a fraction of the overall brain connectivity strength available for the considered subject. The integrated connection density W did not differ between the two groups (Supporting Information Fig. S4). The present choice for the connection weights allowed focusing on the topological organization of each subject brain network, and disentangles dependencies between measures of network organization and total connectivity weight [van Wijk et al., 2010]. No difference was present in term of network density, that is, fraction of existing edges over the maximum number of possible edges in the graph (Supporting Information Table S2).

For some analyses, we used a quantitative measure of structural connectivity that was constructed as follows. For each connecting tract the average generalized fractional anisotropy (gFA) [Tuch, 2004] and average apparent diffusion coefficient (ADC) [Sener, 2001] were computed. These measures are known to be markers of tract integrity, such as axonal packing and myelination levels [Beaulieu, 2002; Takahashi et al., 2002]. To capture the relative importance of tracts sizes we took a similar approach to previous works [Fischi-Gómez et al., 2014; Hagmann et al., 2010a], and weighted the gFA and (inverse) ADC values along each tract by the number of fibers n_{uv} belonging to the tract (u,v) itself.

Network Analysis

For each subject's connectome, global and local weighted network measures describing integration and segregation properties of the brain topology were computed. All the analyses were performed using MATLAB 8.0, The MathWorks, and the Brain Connectivity Toolbox [Rubinov and Sporns, 2010; Sporns, 2011].

Network integration was quantified through the global efficiency [Latora and Marchiori, 2001] and the nodal closeness centrality [Freeman, 1978]. In brief, the global efficiency is inversely proportional to the network characteristic path length, and describes the level of integration of communication between distant parts of the brain network. The nodal closeness centrality is a local measure of centrality, proportional to the inverse average shortest path length between the considered node and all the other brain regions. Segregation properties were quantified through the network transitivity [Newman, 2003] and the nodal local efficiency [Latora and Marchiori, 2001]. The transitivity measure expresses the average level of local connectedness in the network [Opsahl and Panzarasa, 2009], and compared to other segregation measures (e.g., clustering coefficient) is robust with respect to low-strength nodes contribution [Rubinov and Sporns, 2010; Watts and Strogatz, 1998]. The nodal local efficiency describes the degree of connectedness between the regions neighbor of the considered node. These different measures were chosen because of their relevance in describing small-world networks [Bassett and Bullmore, 2006; Latora and Marchiori, 2001; Rubinov and Sporns, 2010]. Taken together, these measures allowed indentifying a distributed set of brain nodes affected in schizophrenia patients. Specifically, in the framework of this study, the affected core of the schizophrenia brain network was defined as the set of nodes presenting significantly decreased values of closeness centrality (integration property) or local efficiency (segregation property) compared to controls. As reported below, the affected core included 26 out of 82 brain nodes.

An investigation of the closeness centrality measure allowed identifying brain hubs, typically defined as the nodes whose centrality measure is significantly higher than on average [Sporns et al., 2007; van den Heuvel and Sporns, 2011]. In this study, normal brain hubs were identified in the control group as the set of nodes presenting a closeness centrality larger than the mean closeness centrality over the whole 82 brain nodes, plus one standard deviation (Fig. 3). Moreover, for each control subject and for each patient, the centrality ranking position (i.e., ordering number) of each node was evaluated with respect to the overall, group-wise nodes ranking based on the closeness centrality values (Fig. 3).

Subnetwork Analysis

Targeted and random attacks have been extensively used in connectome analyses, particularly as a model to

understand the relevance of localized brain damages [Alstott et al., 2009; Bullmore and Sporns, 2009; Kaiser et al., 2007]. In this study, we combined targeted and random attacks to assess the degree of centrality of a specific set of nodes within the overall brain network. In this context, we refer to the degree of centrality of a set of nodes as its topological relevance for the maintenance of the overall network efficiency. The effect of a targeted attack toward a specific set of brain nodes was quantified in relation to a reference distribution estimated from repeated random attacks of nodes. Each attack entailed the removal of a given set of nodes from the network, together with all their connections.

Particularly, the topological role of the affected core was assessed by performing a selective deletion of the entire a-core (targeted attack) from each subject's connectome, and then by computing the efficiency measure within the surviving network. The efficiency of the network under attack that is, measured within the surviving nodes and edges, characterizes the importance of the removed nodes with respect to the overall network communication [Crucitti et al., 2003]. The efficiency of the surviving network was compared with a reference distribution of efficiency values obtained after repeated random attacks (Fig. 4). For each subject, the standard score of the efficiency after targeted attack relative to the efficiency distribution after random attack quantifies the topological centrality of the investigated subnetwork within the overall brain network. A standard score significantly lower than zero indicates that the targeted attack toward the specific subnetwork is more deleterious than by chance.

To estimate the efficiency reference distribution, the null model for the random attack was matched with the targeted attack in terms of (i) number of removed nodes and (ii) overall removed connectivity strength. For each subject, we first removed 26 randomly selected nodes together with their edges; and then if necessary, removed additional edges to match, up to a certain tolerance σ , the overall connectivity strength removed during the targeted attack toward the a-core. In this way, the subject-wise amount of damage, quantified in terms of removed number of nodes and total strength, remains identical across conditions. The tolerance σ was set to one standard deviation of the efficiency values after targeted attack, computed over all the subjects. During node and edge removal, we controlled for network disconnectedness, that is, none of the 56-nodes surviving network was disconnected. The random attack was repeated 1,000 times per subject.

Furthermore, the affected core was quantitatively characterized by computing (i) the number of shortest paths crossing the a-core and (ii) the average connection strength over the edges connecting a-core nodes.

A shortest path is the geodesic path connecting two brain regions and represents a probable pathway of communication [Bullmore and Sporns, 2012; van den Heuvel

et al., 2012]. All the brain network shortest paths were evaluated. Subgroups of the whole-brain shortest paths layout were then considered: (i) paths connecting nodes not belonging to the a-core and passing through the a-core, and (ii) paths connecting nodes not belonging to the a-core but passing through the a-core. A path was defined to pass through the a-core if it involved at least one step within it.

The connection strength averaged within and outside the affected core was quantified in terms of normalized connection density w , gFA, and ADC.

Between Group Comparison

Between-group statistical differences of network and connectivity measures defined in the previous paragraphs were evaluated using the nonparametric Mann-Whitney-Wilcoxon (MWW) test [Wolfe, 2012], setting the significance level α at 0.05. When necessary (for instance, when testing node-wise closeness centrality, local efficiency, and centrality ranking) multiple comparison correction was applied by controlling the false discovery rate (FDR) at $\alpha = 0.05$ [Benjamini and Hochberg, 1995; Meskaldji et al., 2013]. The null hypothesis that the efficiency standard scores (from targeted and random attack comparison) of each group of subjects come from a distribution whose median is zero was tested with the nonparametric Wilcoxon signed-rank (WSR) test [Wilcoxon, 1945]. The correlation between the node centrality rankings of the two groups was evaluated with the Spearman's rank correlation coefficient.

To limit the effect of possible confounding factors, the two groups of subjects were carefully matched by age, gender, and handedness (Supporting Information Table S1). Accordingly, covarying by these three variables did not change the outcomes of the statistical tests performed in this study.

Previous studies suggested a possible relationship between grey and white matter alterations and medication [Moncrieff and Leo, 2010; Smieskova et al., 2009; Szeszko et al., 2014]. The relationship between all the network measures evaluated in this study and the CPZ dose equivalents were assessed for the schizophrenia patients group with the Spearman's rank correlation coefficient.

RESULTS

Identification of Brain Regions Affected in Schizophrenia

First, global integration and segregation properties of the brain connectivity network were investigated in patients and healthy subjects. The global efficiency and the transitivity measures were both decreased in patients compared to controls ($P = 0.0086$, $P = 0.0042$) (Fig. 1). Thereafter, local integration and segregation properties were

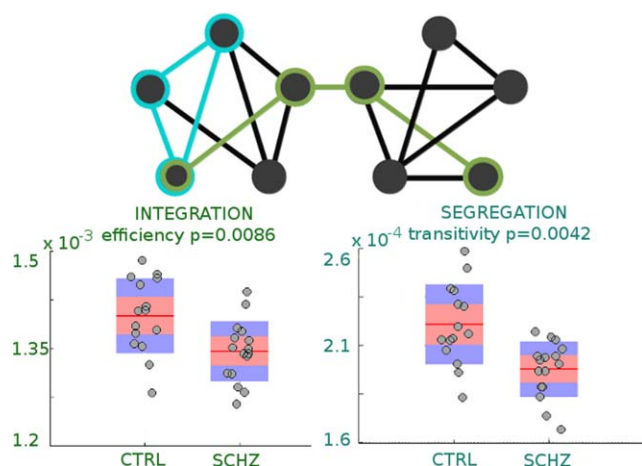


Figure 1.

Integration and segregation deficit in schizophrenia brain networks. First row: schematic representation of network integration and segregation aspects [Bullmore and Sporns, 2009]. The green line highlights the shortest path between two distant nodes; the blue line highlights a local triangle. Second row: box plots representing global network measures dispersion for 16 chronic schizophrenia patients (SCHZ), and 15 healthy controls (CTRL). The red line represents the group mean; the pink area represents the 95% confidence interval. *P*-values from two-side MWW tests are reported.

assessed. To identify the brain regions that mostly contribute to the loss of global topological properties, the single nodes were tested for decreased closeness centrality and decreased local efficiency (one-side MWW test).

The investigation of the local integration and segregation properties allowed identifying a set of nodes compromised in schizophrenia. Such affected core was defined as the set of nodes presenting a significant decrease in nodal closeness centrality or local efficiency, surviving multiple comparison correction at $FDR = 0.05$. The affected core (a-core in the sequel) included fronto-basal (bilateral medial orbitofrontal and left lateral orbitofrontal), middle frontal (bilateral caudal middle frontal and right rostral middle frontal), and inferior frontal (right pars triangularis, left pars orbitalis and left pars opercularis) cortices, left precentral cortex, parietal (bilateral postcentral region, right supramarginal, and precuneus, left superiorparietal) and left temporal-occipital (lateral occipital, middle temporal, and inferior temporal) areas, the basal ganglia (bilateral caudate, pallidum, and accumbens areas, right putamen), and the left thalamus. Figure 2 shows the *FDR*-corrected *P*-values from closeness centrality comparisons for the cortical regions belonging to the affected core. Local efficiency and closeness centrality values for the a-core regions are as well reported in Supporting Information Table S3, together with their between-group statistics.

The affected core encompassed 26 regions involving approximately 30% of the whole brain network nodes.

There was no evidence for increased nodal closeness centrality or local efficiency in patients compared to controls in any of the 82 cortical and subcortical regions.

Topological Role of the Affected Core

To further investigate the brain network organization and the role of the identified a-core within the overall brain topology, we studied the degree of centrality of the different brain regions within the individual brain networks. Particularly, brain nodes were ranked according to their closeness centrality values to identify hubs regions [Sporns et al., 2007], and to evaluate the topological position of the a-core regions within the overall brain network. Figure 3a represents the nodal closeness centrality values for the control group in decreasing order. Regions belonging to the affected core are represented in darker colors. To compare the nodal ranking position between the two groups, the ordering position of each node within the subject-wise closeness centrality ranking was evaluated and compared between the two groups. Moreover, the Spearman's rank correlation coefficient *s* between the two group-wise average rankings was computed. No significant difference in terms of nodes ranking was found between the two groups (node-wise MWW test, $\alpha = 0.05$, $FDR = 0.05$); the Spearman's rank correlation coefficient between the group-wise average ranking of the nodes was $s = 0.94$ ($P = e^{-19}$) for both hemispheres considered separately. Eleven of the 26 a-core regions (approximately 40%

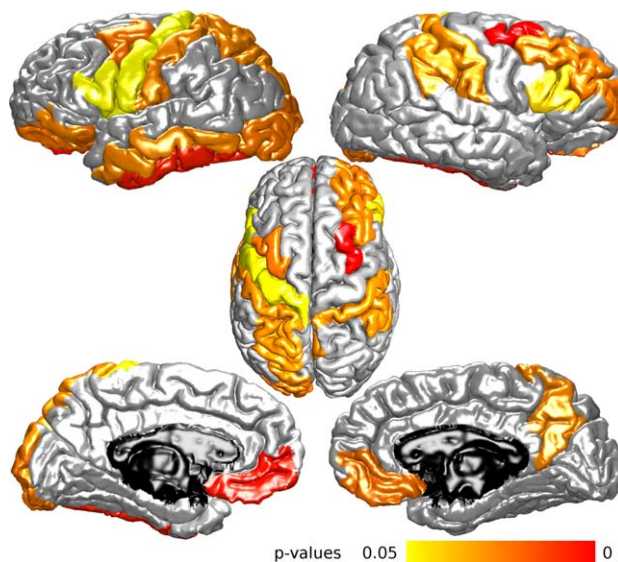


Figure 2.

Surface representation of the cortical areas belonging to the affected core (in color), that is, presenting an alteration of segregation and/or integration properties. Colormap: *P*-values of significantly decreased closeness centrality (one-side MWW test), corrected for multiple comparison ($FDR \alpha = 0.05$).

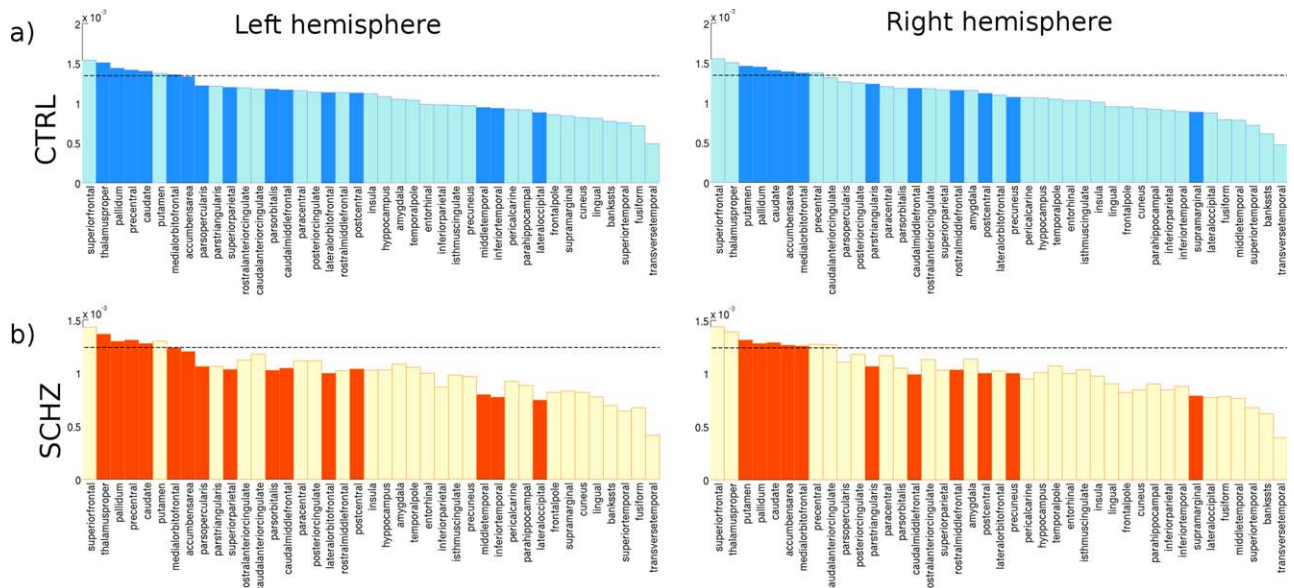


Figure 3.

Nodes ranking according to the average closeness centrality values, for the two hemispheres. Hubs nodes are concentrated on the left of the bar plot. Dark bars represent nodes belonging to the affected subnetwork. The dotted line represents the mean closeness centrality value plus one standard deviation, for each

one of the two groups. **a)** Nodes ranking for the control subjects group. **b)** Average closeness centrality values for the schizophrenia patients group, ordered according to the control subjects nodal ranking.

of the a-core) positioned themselves among the most central brain nodes (hubs), while the other regions of the a-core were more peripheral.

We next examined the degree of centrality of the affected core within the overall brain network. A series of targeted and random attacks directed toward the a-core itself, and toward an equal number of randomly selected

nodes were performed. The null model for the random attack balanced the total strength removed for each subject-wise targeted attack as described above. After each attack, the efficiency of the network surviving the attack was computed. The repetition of 1,000 random attacks allowed evaluating a reference distribution for the efficiency values computed within the surviving network. The

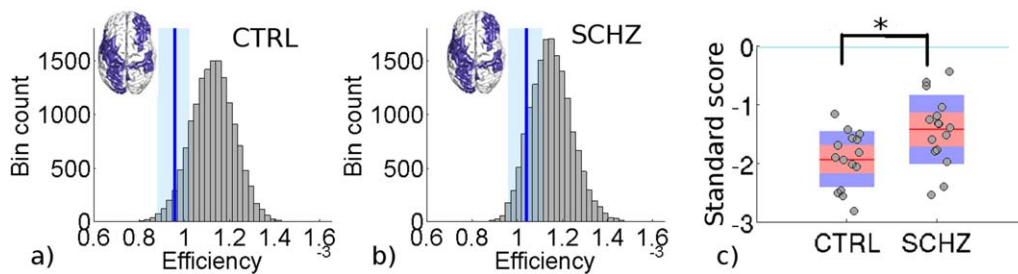


Figure 4.

Effect of random and targeted attack on healthy subjects and schizophrenia patients brain networks. **a,b)** Histograms representing the group-wise distributions of the efficiency values computed after 1,000 repetitions of a random attacks matched to the a-core targeted attack. The random attack was repeated 1,000 times *per* subject. a) control group; b) schizophrenia patients group. The blue lines and light blue areas represent the

mean efficiency values after targeted attack toward the a-core, ± 1 standard deviation, for the two groups. **c)** Box plots representing the efficiency standard scores after targeted attack compared to the reference distribution, for the two groups. The reported *P*-value refers to group comparison (MWW test). Efficiency standard scores were significantly smaller than zero for both groups.

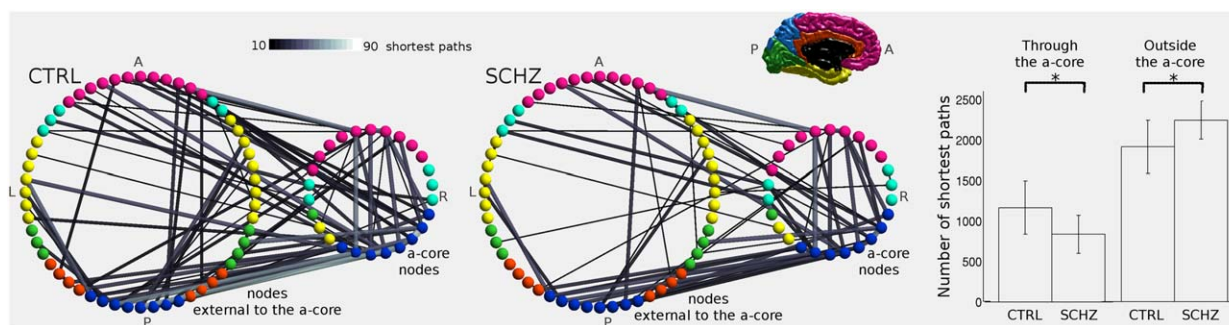


Figure 5.

Communication pathways throughout the affected core. The figure represents the average shortest paths layout between nodes not belonging to the affected core, for healthy controls (CTRL) and schizophrenia patients (SCHZ). Only shortest paths between nodes not belonging to the a-core, but passing through the a-core, are represented. The edge color and thickness represent the number of shortest paths passing through the specific edge, averaged over the two groups of subjects. The nodes are grouped according to their a-

core membership, and color-coded according to their lobe membership. It is possible to visually appreciate that the average number of shortest paths passing through the a-core is decreased in patients compared to controls. The bar plot reports the number of shortest paths between nodes not belonging to the a-core, and passing or not passing through the a-core (group-wise median values \pm 1 standard deviation). * indicates significant between-group difference.

efficiency after the targeted attack was compared to the subject-wise reference distribution by computing its standard scores. Figure 4 shows the efficiency reference distribution after random nodes removal, for the two groups. The efficiency standard score was significantly lower than zero for both groups (WSR test $P < 0.0002$) (Fig. 4), indicating that a targeted attack toward the affected core nodes had a more severe impact on the overall brain communication capacity than a random attack toward an equal number of nodes of similar strength. This means that the a-core has a particular role in maintaining the global efficiency of the network. Moreover, the efficiency standard score was higher (closer to zero) in patients compared to controls ($P = 0.01$) (Fig. 4). Since in patients the a-core is already weakened compared to controls, the impact of a targeted attack is less harmful in patients than in controls.

Finally, the shortest paths layout related to the affected core was compared between the two groups of subjects. A shortest path is a favorable path, in terms of network distance, between two brain regions, and represents a probable pathway of communication between two nodes [Bullmore and Sporns, 2012; van den Heuvel et al., 2012].

Considering the shortest paths connecting nodes external to the a-core only, the number of paths passing through the a-core was decreased in patients compared to controls ($P = 0.008$); on the contrary, the number of shortest paths not passing through the a-core was increased in patients ($P = 0.008$) (Fig. 5). These findings are in line with the definition of the a-core (decreased closeness centrality and local efficiency), and highlight an alteration of the communication pathways, as represented by shortest paths, in schizophrenia patients.

Main results related to the identified affected core held as well when no normalization by streamline length was

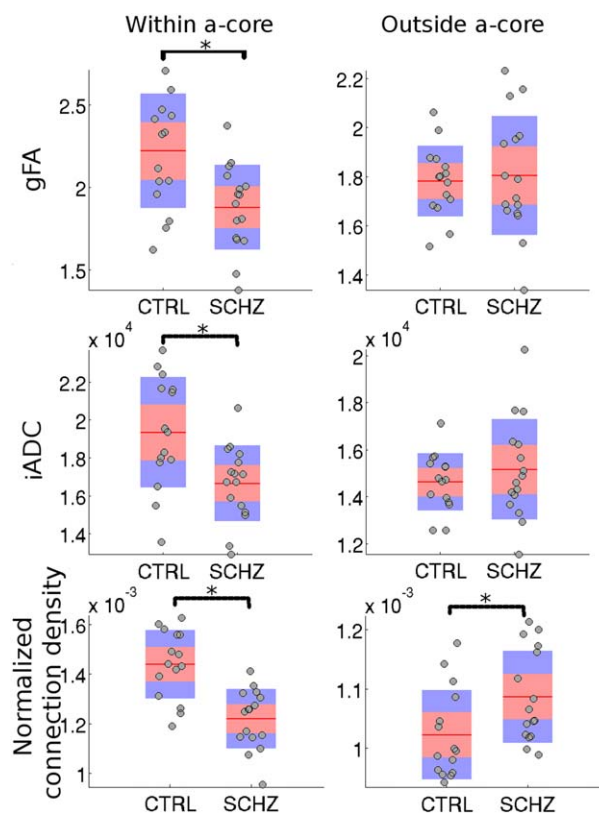


Figure 6.

Box plots representing values dispersion for connectivity strength metrics averaged within (left column) and outside (right column) the affected core. The following metrics are reported: gFA weighted by the size of the tracts (number of fibers); inverse ADC weighted by the size of the tracts; normalized connection density. * indicates significant between-group difference.

applied to the computation of the connectivity weights (Supporting Information Fig. S3).

Characterization of the Affected Core in Schizophrenia Patients

The affected core of schizophrenia brain network was identified as the set of regions showing decreased integration or segregation properties. The a-core includes hubs and peripheral regions, and plays an important role for the achievement of high global network efficiency. The centrality of the affected core is compromised in schizophrenia patients.

To further characterize the affected core and the white matter tracts connecting a-core regions, the connectivity strength within and outside the affected core was estimated and compared between the two groups. The connectivity strength between pairs of brain regions was quantified using three different metrics: (i) normalized connection density (w), (ii) gFA, and (iii) ADC. The three measures were averaged over all the connections between a-core regions (“within a-core”), and over all the connections between regions not belonging to the a-core (“outside a-core”).

The normalized connection density represents the amount of connectivity resources available for a particular connection or subnetwork. The normalized connection density within the a-core was decreased in patients compared to controls ($P = 0.00035$); consequently, the normalized connection density outside the a-core was increased in patients compared to controls ($P = 0.017$) (Fig. 6) (Supporting Information Table S2). This finding is in line with the previous results reported in this study, and demonstrates a redistribution of connectivity resources which favors the a-core regions.

To capture the importance of tract size, gFA and ADC values were weighted by the tract size, expressed as number of fibers. The weighted gFA and the weighted inverse ADC were altered in patients compared to controls when averaged within the a-core (decreased gFA, $P = 0.0076$; decreased iADC, $P = 0.0042$). No between-group difference was found when considering the average gFA and iADC over the connections external to the a-core (Fig. 6). Average connectivity strength values and relative statistics are reported in Supporting Information Table S2.

No correlation was found between any connectivity measure considered in this Results section and the CPZ equivalent dose.

DISCUSSION

The main contribution of this study is to further characterize the connectome in schizophrenia with (i) the identification of a distributed set of affected regions (the affected core or a-core), mainly responsible for the loss of global integration and segregation network properties; (ii) the topological characterization of this affected core within the

overall brain network; and (iii) the investigation of white matter markers along the affected core tracts. These points are discussed in the following.

Based on the brain probability map of Figure 2, we observe that schizophrenia affects connectivity in large parts of prefrontal, pericentral, superior parietal areas, and striatum in both hemispheres, as well as left temporo-occipital and thalamic areas, which is in good agreement with previous literature of grey and white matter alterations (see for instance, [Canu et al., 2014; Shepherd et al., 2012; van den Heuvel et al., 2010; Zalesky et al., 2011]). By definition the affected core comprises regions presenting a decrease of local integration and segregation properties (surviving FDR correction), with a preponderance of integration disruption (Supporting Information Table S3). These nodes exhibit the strongest altered connectivity patterns (dysconnectivity), and accordingly play a major role with respect to the decline of the global topological properties observed in patients.

At the global level the schizophrenia connectome exhibited decreased network efficiency, indicating an overall deficit of functional integration in the network, and in agreement with abundant literature [van den Heuvel and Fornito, 2014]. The transitivity measure was as well decreased in patients compared to controls, indicating an overall altered level of local connectedness. Various diffusion-based studies reported a less integrated and more segregated network in schizophrenia [van den Heuvel and Fornito, 2014]. A tendency toward increased or unchanged overall clustering coefficient has also been reported [Zalesky et al., 2011]. In the present study no brain region showed an increased level of segregation in patients compared to controls. Discrepancies between studies might be attributed to the use of different imaging sequences, different edge weights or different network binarization strategies.

The affected core identified in this study includes parts of the DMN [Greicius et al., 2009] (medial prefrontal regions), of the rich-club [van den Heuvel et al., 2012] (right precuneus and left superior parietal cortex), and of high degree cores of the human connectome [Hagmann et al., 2008; van den Heuvel and Sporns, 2011], particularly subcortical and medial orbitofrontal structures (Supporting Information Table S3). The rich-club and hub nodes have already been shown to be centrally and disproportionately involved in the pathology compared to non-hub regions [Crossley et al., 2014; Rubinov and Bullmore, 2013; van den Heuvel and Fornito, 2014].

In this study, the nodes hubness was investigated by analyzing the nodes ranking in terms of closeness centrality. Hubs can be identified as the nodes whose centrality measure (here: closeness centrality) exceeds the average value of at least one standard deviation [Sporns et al., 2007; van den Heuvel and Sporns, 2011]. Figure 3 illustrates the position of the a-core regions within the centrality ranking of the brain network nodes, with dot lines indicating mean closeness centrality values plus one

standard deviation. According to the considered hub definition, the affected core includes 10 of the 15 hubs (approximately 65% of the whole network hubs), and 16 of the 67 non-hub regions (approximately 25% of the whole network non-hub nodes). Therefore, reported results confirm that hub regions are disproportionately affected in schizophrenia compared to non-hub regions. Moreover, it is noteworthy to observe that a-core nodes do concentrate over the left part of the closeness centrality histogram (higher centrality nodes), but also span toward the lower-centrality area on the right parts of the histogram, therefore including less central (more peripheral) nodes. As such, these findings corroborate the idea that schizophrenia is characterized by the breakdown of distributed brain circuits with a preponderant involvement of central brain nodes, and including as well more peripheral nodes, all contributing to the decrease of communication efficiency (Fig. 4). Significant pathophysiological hypotheses link schizophrenia with the high vulnerability of brain network hubs to metabolic insults [Bullmore and Sporns, 2012; Do et al., 2009; Rubinov and Bullmore, 2013]. Additional complex, yet unknown, factors might explain the involvement of non-hub regions. Our findings suggest that schizophrenia might be not solely, or not specifically a hub disease.

Despite the weakening of highly central brain areas, the investigation of the nodes centrality ranking (Fig. 3) did not highlight any severe reorganization of the nodes centrality hierarchy. None of the brain nodes presented an altered position within the centrality ranking when comparing the two groups. Nevertheless, different aspects of the brain network topological organization in schizophrenia could be highlighted through the characterization of the affected core and related shortest paths (Fig. 5). The affected core plays a distinct role in the maintenance of the brain network communication capacities, in healthy and in schizophrenia subjects, since its removal has a stronger than random effect on global efficiency of communication. As defined in this study, the efficiency standard score quantifies the severity of the impact of a targeted attack against the a-core, compared to a random attack. An efficiency standard score lower than zero was observed in both control and patient groups, indicating that the communication centrality of the affected core was higher than expected by chance. Furthermore, the harmful impact of a targeted attack toward the affected core was significantly more severe in healthy subjects than in patients. These results highlight the fact that removing nodes that already suffer dysconnectivity has a smaller impact than when the removed nodes have normal connectivity (Fig. 4).

The brain network organization observed in the investigated schizophrenia cohort is characterized by an alteration of the shortest paths layout, and by a redistribution of the relative connection weights. The number of shortest paths passing through the affected core was decreased in patients compared to controls (Fig. 5). The normalized connectivity strength, that is, the relative amount of connectivity resources dedicated to a particular connection or subnetwork, was

as well decreased in patients compared to controls when averaged within the affected core (Fig. 6). In general, these findings indicate a weakening of the functional role of the identified affected core with respect to the global brain network communication. This topological configuration leads to less efficient global network topology.

Microstructural white matter alterations could underlie the topological decentralization of the affected core. The alteration of gFA and ADC values along the affected core tracts (Fig. 6) suggests a disruption of white matter properties which could be specific to the affected core circuits (no alteration of gFA and ADC values was found when considering tract external to the a-core). This result suggests and intrinsic microstructural alteration of the a-core white matter regions.

This study has various limitations. First, for most aspects of this report, the connection strength characterization relies on a normalized version of the connectivity density between region pairs. Although the proposed normalization allows focusing on network topology rather than on absolute connectivity strength alterations, and allows reducing the intersubjects variability, it does not directly take into account white matter microstructural properties. Hence, we cannot distinguish whether the observed topological alterations observed in the schizophrenia connectome are related to an intrinsic pathology of the white matter, to an imbalance and redistribution of white matter tracts, and/or to compensatory effects. However, we quantitatively studied the connectivity strength of the a-core with diffusion-based white matter markers (gFA and AD), which were clearly diminished in patients. This result suggests the presence of intrinsic white matter microstructural alterations of the a-core connections. However, the use of more specific, possibly multimodal white matter markers such as magnetization transfer ratio or T2 relaxation [Laule et al., 2007], or new diffusion-based quantitative techniques [Alexander, 2008; Assaf et al., 2013], could potentially address this issue more fully. Second the restricted size of the sample limits the statistical power and the expected robustness of the findings. For instance, the reduced number of subjects included in this study may have as a consequence that the size of the affected subnetwork is underestimated. The replication of the presented findings on larger, possibly independent datasets would definitively be desirable. Third, this study offers a partial vision of schizophrenia pathoconnectomics [Rubinov and Bullmore, 2013], focusing on relative network organizational principles, and shortest paths framework. Alternative visions of brain communication mechanisms such as random walk processes [Goñi et al., 2013] could offer new interpretations of pathological configurations.

CONCLUSION

This study characterizes the network topology underlying the disruption of global network communication

capacity observed in schizophrenia. The previously reported loss of global structural network integration is confirmed. A set of distributed nodes, which drive this global efficiency loss in patients, is identified as the affected core of schizophrenia. Through the failure of these core nodes the topology of the schizophrenia connectome is modified in a way that the shortest path layout is redistributed yielding a more decentralized network. The affected core of patients is characterized by microstructural changes of its connections as measured with gFA and inverse ADC leading to the above described topological changes.

REFERENCES

- Alexander DC (2008): A general framework for experiment design in diffusion MRI and its application in measuring direct tissue-microstructure features. *Magn Reson Med* 60:439–448.
- Alstott J, Breakspear M, Hagmann P, Cammoun L, Sporns O (2009): Modeling the impact of lesions in the human brain. *PLoS Comput Biol* 5:e1000408.
- American Psychiatric Association (2000): Diagnostic and Statistical Manual of Mental Disorders, 4th ed. DSM-IV-TR®. American Psychiatric Pub, Arlington, VA22209, USA.
- Andreasen NC, Pressler M, Nopoulos P, Miller D, Ho B-C (2010): Antipsychotic dose equivalents and dose-years: A standardized method for comparing exposure to different drugs. *Biol Psychiatry* 67:255–262.
- Assaf Y, Alexander DC, Jones DK, Bizzi A, Behrens TEJ, Clark CA, Cohen Y, Dyrby TB, Huppi PS, Knösche TR, LeBihan D, Parker GJM, Poupon C (2013): The CONNECT project: Combining macro- and micro-structure. *NeuroImage* 80:273–282.
- Bassett DS, Bullmore E (2006): Small-world brain networks. *Neuroscientist* 12:512–523.
- Bassett DS, Bullmore E, Verchinski BA, Mattay VS, Weinberger DR, Meyer-Lindenberg A (2008): Hierarchical organization of human cortical networks in health and schizophrenia. *J Neurosci* 28:9239–9248.
- Baumann PS, Cammoun L, Conus P, Do KQ, Marquet P, Meskaldji D, Meuli R, Thiran J-P, Hagmann P (2012): High b-value diffusion-weighted imaging: A sensitive method to reveal white matter differences in schizophrenia. *Psychiatry Res Neuroimaging* 201:144–151.
- Beaulieu C (2002): The basis of anisotropic water diffusion in the nervous system—A technical review. *NMR Biomed* 15:435–455.
- Benjamini Y, Hochberg Y (1995): Controlling the false discovery rate: A practical and powerful approach to multiple testing. *J R Stat Soc Ser B Methodol* 57:289–300.
- Bora E, Fornito A, Radua J, Walterfang M, Seal M, Wood SJ, Yücel M, Velakoulis D, Pantelis C (2011): Neuroanatomical abnormalities in schizophrenia: A multimodal voxelwise meta-analysis and meta-regression analysis. *Schizophr Res* 127:46–57.
- Bullmore E, Sporns O (2009): Complex brain networks: Graph theoretical analysis of structural and functional systems. *Nat Rev Neurosci* 10:186–198.
- Bullmore E, Sporns O (2012): The economy of brain network organization. *Nat Rev Neurosci* 13:336–349.
- Bullmore ET, Bassett DS (2011): Brain graphs: Graphical models of the human brain connectome. *Annu Rev Clin Psychol* 7:113–140.
- Cammoun L, Gigandet X, Meskaldji D, Thiran JP, Sporns O, Do KQ, Maeder P, Meuli R, Hagmann P (2012): Mapping the human connectome at multiple scales with diffusion spectrum MRI. *J Neurosci Methods* 203:386–397.
- Canu E, Agosta F, Filippi M (2014): A selective review of structural connectivity abnormalities of schizophrenic patients at different stages of the disease. *Schizophr Res*. Available online 2 June 2014 at: <http://www.sciencedirect.com/science/article/pii/S0920996414002527>.
- Collin G, Kahn RS, Reus MA de, Cahn W, Heuvel MP van den (2013): Impaired rich club connectivity in unaffected siblings of schizophrenia patients. *Schizophr Bull* 40:438–448.
- Crossley NA, Mechelli A, Scott J, Carletti F, Fox PT, McGuire P, Bullmore ET (2014): The hubs of the human connectome are generally implicated in the anatomy of brain disorders. *Brain* 137:2382–2395.
- Crucitti P, Latora V, Marchiori M, Rapisarda A (2003): Efficiency of scale-free networks: Error and attack tolerance. *Phys Stat Mech Appl* 320:622–642.
- Daducci A, Gerhard S, Griffa A, Lemkaddem A, Cammoun L, Gigandet X, Meuli R, Hagmann P, Thiran J-P (2012): The connectome mapper: An open-source processing pipeline to map connectomes with MRI. *PLoS One* 7:e48121.
- Damoiseaux JS, Smith SM, Witter MP, Sanz-Arigita EJ, Barkhof F, Scheltens P, Stam CJ, Zarei M, Rombouts SARB (2009): White matter tract integrity in aging and Alzheimer’s disease. *Hum Brain Mapp* 30:1051–1059.
- Desikan RS, Ségonne F, Fischl B, Quinn BT, Dickerson BC, Blacker D, Buckner RL, Dale AM, Maguire RP, Hyman BT, Albert MS, Killiany RJ (2006): An automated labeling system for subdividing the human cerebral cortex on MRI scans into gyral based regions of interest. *Neuroimage* 31:968–980.
- Do KQ, Cabungcal JH, Frank A, Steullet P, Cuenod M (2009): Redox dysregulation, neurodevelopment, and schizophrenia. *Curr Opin Neurobiol* 19:220–230.
- Drzezga A, Becker JA, Dijk KRAV, Sreenivasan A, Talukdar T, Sullivan C, Schultz AP, Sepulcre J, Putcha D, Greve D, Johnson KA, Sperlring RA (2011): Neuronal dysfunction and disconnection of cortical hubs in non-demented subjects with elevated amyloid burden. *Brain* 134:1635–1646.
- Ellison-Wright I, Bullmore E (2009): Meta-analysis of diffusion tensor imaging studies in schizophrenia. *Schizophr Res* 108:3–10.
- Filippi M, Heuvel MP van den, Fornito A, He Y, Hulshoff Pol HE, Agosta F, Comi G, Rocca MA (2013): Assessment of system dysfunction in the brain through MRI-based connectomics. *Lancet Neurol* 12:1189–1199.
- Fischi-Gómez E, Vasung L, Meskaldji D-E, Lazeyras F, Borradori-Tolsa C, Hagmann P, Barisnikov K, Thiran J-P, Hüppi PS (2014): Structural brain connectivity in school-age preterm infants provides evidence for impaired networks relevant for higher order cognitive skills and social cognition. *Cereb Cortex* bhu073.
- Fitzsimmons J, Kubicki M, Shenton ME (2013): Review of functional and anatomical brain connectivity findings in schizophrenia. *Curr Opin Psychiatry* 26:172–187.
- Fornito A, Zalesky A, Pantelis C, Bullmore ET (2012): Schizophrenia, neuroimaging and connectomics. *NeuroImage* 62:2296–2314.

- Freeman LC (1978): Centrality in social networks conceptual clarification. *Soc Netw* 1:215–239.
- Friston KJ, Frith CD (1995): Schizophrenia: a disconnection syndrome? *Clin Neurosci* 3:89–97.
- Gigandet X, Griffa A, Kober T, Daducci A, Gilbert G, Connelly A, Hagmann P, Meuli R, Thiran J-P, Krueger G (2013): A connectome-based comparison of diffusion mri schemes. *PLoS One* 8:e75061.
- Glahn DC, Laird AR, Ellison-Wright I, Thelen SM, Robinson JL, Lancaster JL, Bullmore E, Fox PT (2008): Meta-analysis of gray matter anomalies in schizophrenia: Application of anatomic likelihood estimation and network analysis. *Biol Psychiatry* 64:774–781.
- Goni J, Avena-Koenigsberger A, Velez de Mendizabal N, Heuvel MP, van den, Betzel RF, Sporns O (2013): Exploring the morphospace of communication efficiency in complex networks. *PLoS One* 8:e58070.
- Greicius MD, Supekar K, Menon V, Dougherty RF (2009): Resting-state functional connectivity reflects structural connectivity in the default mode network. *Cereb Cortex* 19:72–78.
- Griffa A, Baumann PS, Thiran J-P, Hagmann P (2013): Structural connectomics in brain diseases. *NeuroImage* 80:515–526.
- Guye M, Bettus G, Bartolomei F, Cozzone PJ (2010): Graph theoretical analysis of structural and functional connectivity MRI in normal and pathological brain networks. *Magn Reson Mater Phys Biol Med* 23:409–421.
- Hagmann Patric (2005): From diffusion MRI to brain connectomics. Lausanne: EPFL. 141 pages. Available at: <http://infoscience.epfl.ch/record/33696>.
- Hagmann P, Cammoun L, Gigandet X, Meuli R, Honey CJ, Wedeen VJ, Sporns O (2008): Mapping the Structural Core of Human Cerebral Cortex. *PLoS Biol* 6:e159.
- Hagmann P, Sporns O, Madan N, Cammoun L, Pienaar R, Wedeen VJ, Meuli R, Thiran J-P, Grant PE (2010a): White matter maturation reshapes structural connectivity in the late developing human brain. *Proc Natl Acad Sci USA* 107:19067–19072.
- Hagmann P, Cammoun L, Gigandet X, Gerhard S, Grant PE, Wedeen V, Meuli R, Thiran J-P, Honey CJ, Sporns O (2010b): MR connectomics: Principles and challenges. *J Neurosci Methods* 194:34–45.
- Honea R, Crow TJ, Passingham D, Mackay CE (2005): Regional deficits in brain volume in schizophrenia: A meta-analysis of voxel-based morphometry studies. *Am J Psychiatry* 162:2233–2245.
- Kaiser M, Martin R, Andras P, Young MP (2007): Simulation of robustness against lesions of cortical networks. *Eur J Neurosci* 25:3185–3192.
- Latora V, Marchiori M (2001): Efficient Behavior of Small-World Networks. *Phys Rev Lett* 87:198701.
- Laule C, Vavasour IM, Kolind SH, Li DKB, Traboulsee TL, Moore GRW, MacKay AL (2007): Magnetic resonance imaging of myelin. *Neurotherapeutics* 4:460–484.
- Lo C-Y, Wang P-N, Chou K-H, Wang J, He Y, Lin C-P (2010): Diffusion tensor tractography reveals abnormal topological organization in structural cortical networks in Alzheimer's disease. *J Neurosci* 30:16876–16885.
- Lynall M-E, Bassett DS, Kerwin R, McKenna PJ, Kitzbichler M, Muller U, Bullmore E (2010): functional connectivity and brain networks in schizophrenia. *J Neurosci* 30:9477–9487.
- Mendelsohn A, Strous RD, Bleich M, Assaf Y, Hendler T (2006): Regional axonal abnormalities in first episode schizophrenia: Preliminary evidence based on high b-value diffusion-weighted imaging. *Psychiatry Res Neuroimaging* 146:223–229.
- Meskaldji DE, Fischi-Gomez E, Griffa A, Hagmann P, Morgenthaler S, Thiran J-P (2013): Comparing connectomes across subjects and populations at different scales. *Neuroimage* 80:416–425.
- Moncrieff J, Leo J (2010): A systematic review of the effects of antipsychotic drugs on brain volume. *Psychol Med* 40:1409–1422.
- Mori S, Crain BJ, Chacko V, Van Zijl P (1999): Three-dimensional tracking of axonal projections in the brain by magnetic resonance imaging. *Ann Neurol* 45:265–269.
- Newman MEJ (2003): The Structure and Function of Complex Networks. *SIAM Rev* 45:167–256.
- Oh SW, Harris JA, Ng L, Winslow B, Cain N, Mihalas S, Wang Q, Lau C, Kuan L, Henry AM, Mortrud MT, Ouellette B, Nguyen TN, Sorensen SA, Slaughterbeck CR, Wakeman W, Li Y, Feng D, Ho A, Nicholas E, Hirokawa KE, Bohn P, Joines KM, Peng H, Hawrylycz MJ, Phillips JW, Hohmann JG, Wohnoutka P, Gerfen CR, Koch C, Bernard A, Dang C, Jones AR, Zeng H (2014): A mesoscale connectome of the mouse brain. *Nature* 508:207–214.
- Opsahl T, Panzarasa P (2009): Clustering in weighted networks. *Soc Netw* 31:155–163.
- Ottet M-C, Schaer M, Debbane M, Cammoun L, Thiran J-P, Eliez S (2013): Graph theory reveals disconnected hubs in 22q11DS and altered nodal efficiency in patients with hallucinations. *Front Hum Neurosci* 7:402.
- Pettersson-Yeo W, Allen P, Benetti S, McGuire P, Mechelli A (2011): Dysconnectivity in schizophrenia: Where are we now? *Neurosci Biobehav Rev* 35:1110–1124.
- Preisig M, Fenton BT, Matthey M-L, Berney A, Ferrero F (1999): Diagnostic interview for genetic studies (DIGS): Inter-rater and test-retest reliability of the French version. *Eur Arch Psychiatry Clin Neurosci* 249:174–179.
- Rubinov M, Bullmore E (2013): Fledgling pathoconnectomics of psychiatric disorders. *Trends Cogn Sci* 17:641–647.
- Rubinov M, Sporns O (2010): Complex network measures of brain connectivity: Uses and interpretations. *Neuroimage* 52:1059–1069.
- Sener RN (2001): Diffusion MRI: Apparent diffusion coefficient (ADC) values in the normal brain and a classification of brain disorders based on ADC values. *Comput Med Imaging Graph* 25:299–326.
- Shepherd AM, Laurens KR, Matheson SL, Carr VJ, Green MJ (2012): Systematic meta-review and quality assessment of the structural brain alterations in schizophrenia. *Neurosci Biobehav Rev* 36:1342–1356.
- Skudlarski P, Jagannathan K, Anderson K, Stevens MC, Calhoun VD, Skudlarska BA, Pearlson G (2010): Brain connectivity is not only lower but different in schizophrenia: A combined anatomical and functional approach. *Biol Psychiatry* 68:61–69.
- Smieskova R, Fusar-Poli P, Allen P, Bendfeldt K, Stieglitz RD, Drewe J, Radue EW, McGuire PK, Riecher-Rossler A, Borgwardt SJ (2009): The effects of antipsychotics on the brain: What have we learnt from structural imaging of schizophrenia? A systematic review. *Curr Pharm Des* 15:2535–2549.
- Sporns O (2011): *Networks of the Brain*. MIT Press, Cambridge, MA 02142–1209, USA.
- Sporns O (2013): Network attributes for segregation and integration in the human brain. *Curr Opin Neurobiol* 23:162–171.

- Sporns O, Tononi G, Kötter R (2005): The human connectome: A structural description of the human brain. *PLoS Comput Biol* 1:e42.
- Sporns O, Honey CJ, Kötter R (2007): Identification and classification of hubs in brain networks. *PLoS One* 2:e1049.
- Stephan KE, Baldeweg T, Friston KJ (2006): Synaptic plasticity and dysconnection in schizophrenia. *Biol Psychiatry* 59:929–939.
- Stephan KE, Friston KJ, Frith CD (2009): Dysconnection in schizophrenia: From abnormal synaptic plasticity to failures of self-monitoring. *Schizophr Bull* 35:509–527.
- Szeszko PR, Robinson DG, Ikuta T, Peters BD, Gallego JA, Kane J, Malhotra AK (2014): White matter changes associated with antipsychotic treatment in first-episode psychosis. *Neuropsychopharmacology* 39:1324–1331.
- Takahashi M, Hackney DB, Zhang G, Wehrli SL, Wright AC, O'Brien WT, Uematsu H, Wehrli FW, Selzer ME (2002): Magnetic resonance microimaging of intraaxonal water diffusion in live excised lamprey spinal cord. *Proc Natl Acad Sci USA* 99:16192–16196.
- Tomasi D, Volkow ND (2012): Aging and functional brain networks. *Mol Psychiatry* 17:549–558.
- Tuch DS (2004): Q-ball imaging. *Magn Reson Med* 52:1358–1372.
- Van den Heuvel MP, Fornito A (2014): Brain networks in schizophrenia. *Neuropsychol Rev* 24:32–48.
- Van den Heuvel MP, Sporns O (2011): Rich-club organization of the human connectome. *J Neurosci* 31:15775–15786.
- Van den Heuvel MP, Mandl RCW, Stam CJ, Kahn RS, Pol HEH (2010): Aberrant frontal and temporal complex network structure in schizophrenia: A graph theoretical analysis. *J Neurosci* 30:15915–15926.
- Van den Heuvel MP, Kahn RS, Goñi J, Sporns O (2012): High-cost, high-capacity backbone for global brain communication. *Proc Natl Acad Sci USA* 109:11372–11377.
- Van den Heuvel MP, Sporns O, Collin G, Scheewe T, Mandl RCW, Cahn W, Goñi J, Hulshoff Pol HE, Kahn RS (2013): Abnormal rich club organization and functional brain dynamics in schizophrenia. *JAMA Psychiatry* 70:783–792.
- Van Wijk BCM, Stam CJ, Daffertshofer A (2010): Comparing brain networks of different size and connectivity density using graph theory. *PLoS One* 5:e13701.
- Varoquaux G, Craddock RC (2013): Learning and comparing functional connectomes across subjects. *NeuroImage* 80:405–415.
- Wang Q, Su T-P, Zhou Y, Chou K-H, Chen I-Y, Jiang T, Lin C-P (2012): Anatomical insights into disrupted small-world networks in schizophrenia. *NeuroImage* 59:1085–1093.
- Watts DJ, Strogatz SH (1998): Collective dynamics of “small-world” networks. *Nature* 393:440–442.
- Wedeen VJ, Hagmann P, Tseng W-YI, Reese TG, Weisskoff RM (2005): Mapping complex tissue architecture with diffusion spectrum magnetic resonance imaging. *Magn Reson Med* 54:1377–1386.
- Wedeen VJ, Rosene DL, Wang R, Dai G, Mortazavi F, Hagmann P, Kaas JH, Tseng W-YI (2012): The Geometric Structure of the Brain Fiber Pathways. *Science* 335:1628–1634.
- Wilcoxon F (1945): Individual comparisons by ranking methods. *Biom Bull* 1:80–83.
- Wolfe DA (2012): Nonparametrics: Statistical methods based on ranks and its impact on the field of nonparametric statistics. In: Rojo J, editor. *Selected Works of E. L. Lehmann. Selected Works in Probability and Statistics*. Springer US, Houston, TX77005, USA. pp 1101–1110.
- Yendiki A, Koldewyn K, Kakunoori S, Kanwisher N, Fischl B (2014): Spurious group differences due to head motion in a diffusion MRI study. *Neuroimage* 88:79–90.
- Yu Q, Sui J, Liu J, Plis SM, Kiehl KA, Pearlson G, Calhoun VD (2013): Disrupted correlation between low frequency power and connectivity strength of resting state brain networks in schizophrenia. *Schizophr Res* 143:165–171.
- Zalesky A, Fornito A, Seal ML, Cocchi L, Westin C-F, Bullmore ET, Egan GF, Pantelis C (2011): Disrupted axonal fiber connectivity in schizophrenia. *Biol Psychiatry* 69:80–89.
- Zhang Z, Liao W, Chen H, Mantini D, Ding J-R, Xu Q, Wang Z, Yuan C, Chen G, Jiao Q, Lu G (2011): Altered functional-structural coupling of large-scale brain networks in idiopathic generalized epilepsy. *Brain* 134:2912–2928.
- Zhang Y, Lin L, Lin C-P, Zhou Y, Chou K-H, Lo C-Y, Su T-P, Jiang T (2012): Abnormal topological organization of structural brain networks in schizophrenia. *Schizophr Res* 141:109–118.